

PAPER • OPEN ACCESS

## Data assimilation for the prediction of wake trajectories within wind farms

To cite this article: M Lejeune *et al* 2020 *J. Phys.: Conf. Ser.* **1618** 062055

View the [article online](#) for updates and enhancements.

### You may also like

- [Structure, Kinematics, and Observability of the Large Magellanic Cloud's Dynamical Friction Wake in Cold versus Fuzzy Dark Matter](#)  
Hayden R. Foote, Gurtina Besla, Philip Mocz et al.
- [Phase-difference on seal whisker surface induces hairpin vortices in the wake to suppress force oscillation](#)  
Geng Liu, Qian Xue and Xudong Zheng
- [Effect of axis ratio on unsteady wake of surface mounted elliptic cylinder immersed in shear flow](#)  
Prashant Kumar and Shaligram Tiwari



**ECS**  
The  
Electrochemical  
Society  
Advancing solid state &  
electrochemical science & technology

**DISCOVER**  
how sustainability  
intersects with  
electrochemistry & solid  
state science research

# Data assimilation for the prediction of wake trajectories within wind farms

M Lejeune<sup>1</sup>, M Moens<sup>1</sup>, M Coquelet<sup>1,2</sup>, N Coudou<sup>1,2,3</sup>, P Chatelain<sup>1</sup>

<sup>1</sup> Institute of Mechanics, Materials and Civil Engineering, Université catholique de Louvain, 1348 Louvain-la-Neuve, Belgium

<sup>2</sup> Fluids-Machines Department, Université de Mons, 7000 Mons, Belgium.

<sup>3</sup> von Karman Institute for Fluid Dynamics, 1640 Sint-Genesius-Rode, Belgium

E-mail: [maxime.lejeune@uclouvain.be](mailto:maxime.lejeune@uclouvain.be)

**Abstract.** In this paper, we formulate a physics-based surrogate wake model in the framework of online wind farm control. A flow sensing module is coupled with a wake model in order to predict the behavior of the wake downstream of a wind turbine based on its loads, wind probe data and operating settings. Information about the incoming flow is recovered using flow sensing techniques and then fed to the wake model, which reconstructs the wake based on this limited set of information. Special focus is laid on limiting the number of input parameters while keeping the computational cost low in order to facilitate the tuning procedure. Once calibrated, comparison with high-fidelity numerical results retrieved from Large Eddy Simulation (LES) of a wind farm confirms the good potential of the approach for online wake prediction within farms. The two approaches are further compared in terms of their wake center and time-averaged speed deficit predictions demonstrating good agreement in the process.

## 1. Introduction

The improvement of wind power plants controllers has progressively grown into one of the key approaches envisioned to further reduce the Levelized Cost Of Energy (LCOE) in the context of wind energy. To this end, several strategies have gradually been introduced in an attempt to optimize the power production of wind farms and alleviate loads. However, for most, these strategies have been oriented toward the development of individualistic controllers maximizing the efficiency of isolated wind turbines. This approach, though comparatively simple, fails to consider the wake effects thereby leading to a suboptimal operating point of the wind farm taken as a whole. For this reason, focus has recently shifted toward the development of global controllers designed to track the optimal operating point of wind turbines while accounting for wind turbines interactions.

Selecting the optimal control policy however requires an adequate level of understanding of the wake physics in order to forecast the interactions between neighbouring wind turbines. In model-based wind farm control, the controller relies on a simplified surrogate model in order to evaluate the impact of a control input change on the wake physics and hence on the global performance of the wind power plant. The surrogate model used must therefore satisfy some important criteria: it must be fast enough to be usable in the online control framework while guarantying a sufficient level of faithfulness to the reality. Indeed, an excessive mismatch between the model predictions and the reality could lead to catastrophic performances of the controller,



Content from this work may be used under the terms of the [Creative Commons Attribution 3.0 licence](https://creativecommons.org/licenses/by/3.0/). Any further distribution of this work must maintain attribution to the author(s) and the title of the work, journal citation and DOI.

which could eventually result in a LCOE increase. To this day, the development of accurate surrogate models therefore still remains one of the pivotal challenges faced by the model-based strategy due to the unsteady nature of wind wakes and their high sensitivity to the local wind characteristics.

While modern high-fidelity numerical tools such as Large Eddy Simulation (LES) allow to accurately capture the flow at the wind farm scale, they still come at a prohibitive computational cost preventing their use as surrogate models. To this day, wind farm controller design has thus mostly been relying on the use of low- to medium-fidelity flow models. Low fidelity models are typically based on empirical steady-state wake models (eg: Jensen [1], Bastankhah et al. [2]) and are hence characterized by a low computational cost. They have been receiving a lot of attention from the wind farm control community despite sometimes being criticized for their extensive need for condition-dependent tuning. Further, their lack of physical ground along with its underlying steady state assumption completely overlook some key phenomena such as the wake propagation through the farm although they are of crucial importance for wind farm control. Medium-fidelity wake models (eg: Dynamic Wake Meandering (DWM) model [3] and its FAST-Farm implementation [4]) propose to bridge the gap between expensive high-fidelity LES and fast empirical models by providing a simplified yet reasonably faithful physics-based description of the wake. These models allow to capture well the distinctive dynamic features of the wake while maintaining an affordable computational cost. They however require the tuning of a large set of parameters and assume the knowledge of the incoming flow field.

The aforementioned limitations and especially the need for case-dependent tuning of the low- and medium-fidelity approaches consequently undermine the reliability of their resulting flow prediction when applied over a wide and uncertain spectrum of operating conditions. As a result, a growing interest for the development of online tuning tools allowing the simultaneous update and correction of the underlying surrogate model has emerged in the literature [5, 6, 7]. In [8], Doekemeijer et al. synthesize an online model calibration procedure for a 2D simplified Navier-Stokes solver by feeding an ensemble Kalman filter with power measurements. Schreiber et al. [9] on the other hand, take a more pragmatic approach by using an online maximum likelihood tuning method to retrieve the optimal set of model tuning parameters based on the SCADA data. A common feature of the latter two approaches is that they manage to achieve simultaneous model tuning and flow correction thereby capturing some of the unmodeled physics.

The present work aims to formulate a medium-fidelity surrogate wake model in line with the joint state-parameter estimation framework. The target is thus to develop an unsteady operational model capable of accurately predicting in fast-time the behavior of a wind turbine wake based on its operating settings and on the flow measurements recovered using flow sensing techniques [10]. The resulting model should capture the main features of the wake dynamics while relying on the state-parameter correction approach to account for unmodeled physics. Furthermore, in an attempt to facilitate the online tuning procedure, focus is laid on choosing an appropriate limited set of independent tuning parameters as well as on selecting a concise state description of the flow. This paper thus takes inspiration on the success gathered by FAST-Farm in order to synthesize a medium-fidelity surrogate wake model. However, unlike the classical approach, which assumes the inlet turbulent field to be fully known, it reconstructs the inlet turbulent velocity field from the wind measurements allowing the online estimation of wake propagation in the process. The resulting framework is first presented and then validated against advanced high-fidelity LES of wind farms.

## 2. Methodology

### 2.1. Wake model

The proposed model is based upon the hypothesis, consistent with the frozen turbulence framework, that the wake behaves as a passive tracer advected by the background flow. As

illustrated in Fig. 1, the wake modelization strategy is similar to that used in the FAST-Farm [4] simulation tool: the wake is discretized as a series of wake particles shed at successive time steps and convected by the ambient flow.

A wake particle,  $P_i$ , shed at time  $t_i$ , is described by a position,  $\mathbf{x}_{P_i}(t)$ , an orientation,  $\mathbf{n}_{P_i}(t)$  and a speed deficit field  $\Delta u_{P_i}(t, r_{P_i}(\mathbf{x}))$  where  $r_{P_i}(\mathbf{x})$  and  $t$  denote the radial position of  $\mathbf{x}$  relative to the wake particle and the current time respectively.

The position of the particle,  $\mathbf{x}_{P_i}(t) = x_{P_i}\hat{\mathbf{e}}_{x,WT} + z_{P_i}\hat{\mathbf{e}}_{z,WT}$ , is measured in the wind turbine-fixed frame  $\hat{\mathbf{e}}_{*,WT}$  and initially coincides with that of the wind turbine hub. The particle advection is then handled in a Lagrangian fashion using the wake advection module presented later in this Section. Furthermore, the orientation of the particle,  $\mathbf{n}_{P_i}(t)$ , is introduced to allow the computation of the radial position of an arbitrary point,  $\mathbf{x}$ , in the wake particle frame:

$$r_{P_i}(\mathbf{x}) = \left\| (\mathbf{x} - \mathbf{x}_{P_i}) - (\mathbf{x} - \mathbf{x}_{P_i}) \cdot \mathbf{n}_{P_i} \right\|. \quad (1)$$

Following Bastankhah [2], the speed deficit can then be represented by a Gaussian parametrized in terms of the thrust coefficient,  $C_{T_{P_i}}$ , and the turbulence intensity,  $TI_{P_i}$ , measured at the turbine hub at the shedding time,  $t_i$ :

$$\Delta u_{P_i}(t, r_{P_i}) = U_0 \left( 1 - \sqrt{1 - \frac{C_T}{8(\sigma/D)^2}} \right) \times \exp \left( -\frac{1}{2(\sigma/D)^2} \left( \frac{r_{P_i}}{D} \right)^2 \right) \quad (2)$$

where  $D$  is the diameter of the wind turbine and  $U_0$  the freestream wind speed. The width of the Gaussian,  $\sigma(x_{P_i})$ , is expressed as  $\sigma(x_{P_i}) = k(TI_{P_i}) x_{P_i} + \varepsilon_0 D$ . In order to increase the robustness of the model, the wake growth rate constant,  $k$ , is in turn computed as a linear function of the turbulent intensity,  $TI_{P_i}$  [11, 12]:

$$k(TI_{P_i}) = a_k + b_k TI_{P_i} \quad (3)$$

with  $a_k$  and  $b_k$  tuning constants. This formulation consequently assumes that the wake expansion exclusively depends on the ambient turbulent mixing and therefore neglects some other possibly important mixing contributions such as the ones induced by the tip-vortex breakdown or atmospheric shear. The contribution of the pressure expansion term in the near wake, on the other hand, is still somewhat accounted for by the initial value of the growth rate constant  $\sigma = \varepsilon_0 D$ .

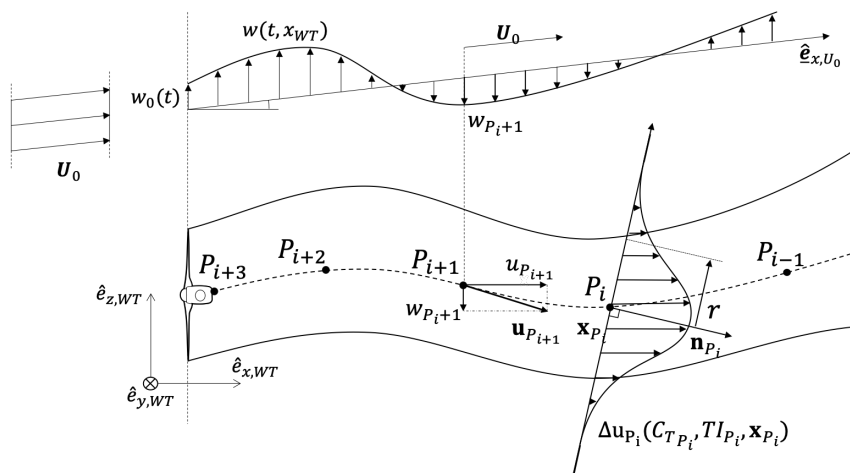


**Figure 1.** Wake discretization strategy

### 2.2. Flow sensing module

The local wind characteristics are estimated by a Kalman filter based on running a Blade Element Momentum code [10] to which the loads and operating settings of the wind turbine are fed. This parametrization allows to eventually fully determine the characteristics of the wake particles and of the freestream flow using the wind turbine measurements only.

The wind turbine blades are essentially considered as moving sensors whose out-of-plane bending loads are strictly connected to the local wind speed at the blade position. The rotor is then divided in  $N_S$  sectors. Doing so allows to recover an estimate of the effective wind speed averaged over each of these sectors, the so-called sector effective wind speed,  $u_{SE}$ . The latter estimate is updated each time a blade crosses the corresponding sector by averaging the measured bending load over the crossing time window. The resulting local wind speed estimations on the different wind turbine sectors can then be combined into  $u_{RE} = \Sigma u_{SE}/N_S$ , the rotor effective wind speed, which, in turn, enables us to directly obtain the corresponding thrust coefficient from the turbine measured thrust,  $T$ :

$$C_{T_{P_i}} = \frac{T(t_i)}{0.5\rho\pi(D/2)^2 u_{RE}^2(t_i)} \quad (4)$$

with  $\rho$  the air density. In a similar fashion, the main features of the incoming wind are recovered as follows:

$$U_0 = (\bar{u}_{RE})_{uw} \quad \text{and} \quad TI_{P_i} = \frac{\bar{s}(u_{SE})}{\bar{u}_{RE}} \quad (5)$$

$s(*)$  denotes the discrete standard deviation operator while the  $\bar{*}$  operator indicates the flow characteristics are averaged over a prescribed time window to ensure their convergence thereby assuming flow features remain relatively steady. Moreover, the estimated freestream velocity is computed from the rotor effective wind speed of the unwaked wind turbines only,  $(*)_{uw}$ . The resulting averaged freestream wind conditions estimated by the unwaked wind turbines are in turn used as the uniform freestream velocity field across the complete simulation domain of the model.

This estimation procedure is applied at time  $t_i$ . The characteristics computed using this method are then immediately fed to the wake particle,  $P_i$ , shed at the corresponding wind turbine hub and timestep.

The simulation domain velocity field is initialized to an uniform field with no wake particule and whose characteristics are provided as parameters. The model initial state should therefore not be trusted since the wake particules need a few convective times (typically  $10D/U_0$  s) to propagate the information downstream thereby advecting the wake.

### 2.3. Wake advection module

The last step consists in updating the positions of the shed wake particles. Classically, this would be done by considering the inflow velocity field as known and then advecting the wake using this field [4, 3]. However, focus is here laid on developing a model that could be used in the context of online control where the incoming turbulent flow field is obviously not available. Advection is thus handled in a Lagrangian fashion where the advection speed,  $\mathbf{u}_{P_i}$ , is decomposed into two components:  $u_{P_i}$  and  $w_{P_i}$ .

The axial convection speed,  $u_{P_i}$ , is readily computed using the speed deficit expression obtained previously:  $u_{P_i}(t) = U_0(t) - c_w \Delta u_{P_i}(t, 0)$  where  $c_w$  is a tuning constant. In the context of multiple superposing wakes, the standard root-sum-square weighting superposition strategy is applied [13, 11]:

$$u_{P_i}(t) = U_0(t) - c_w \sqrt{\sum_{j \in S} \Delta u_{P_j}^2(t, r_{P_j}(\mathbf{x}_{P_i}(t)))} \quad (6)$$

where  $\mathcal{S}$  denotes the set of the closest wake particles for each superposing wake.

In contrast, the transverse velocity field,  $w_{p_i}$ , can not be obtained in such a straightforward fashion and requires an additional modeling hypothesis. The inflow flow field is first assumed to respect the classical frozen turbulence hypothesis. This implies that information about the incoming flow field is conserved along the mean flow streamlines,  $x_{U_0}\hat{\mathbf{e}}_{x,U_0}$ :

$$\frac{\partial w}{\partial t}(x_{U_0}, t) + c_0 U_0(t) \frac{\partial w}{\partial x_{U_0}}(x_{U_0}, t) = 0, \quad (7)$$

where  $c_0 U_0(t)$  is the effective freestream convection speed while  $c_0 < 1.0$  is a tuning constant accounting for the nearby influence of the wake. Integrating Eq. 7 along the mean flow streamline passing through the wind turbine hub can be performed using a standard second order upwind scheme but requires the formulation of a boundary condition. This boundary condition,  $w_0(t)$ , is obtained by probing and then low-pass filtering the transverse speed at the wind turbine hub that would be obtained using a sensor device (eg: pitot tube located on top of the turbine hub). This boundary approach assumes only large turbulent scales are relevant for the meandering phenomenon while it also partially removes the probing noise. A standard exponential window filter is implemented:

$$w_0(t) = \alpha w_0(t - \Delta t) + (1 - \alpha) w_{h, \text{meas}}(t) \quad (8)$$

where  $\alpha$  is the filter time scale and  $w_{h, \text{meas}}(t)$ , the transverse velocity measurement at the wind turbine hub at time  $t$ .

The resulting surrogate wake model thus depends on only five tuning parameters ( $a_k$ ,  $b_k$ ,  $c_w$ ,  $c_0$ , and  $\alpha$ ). Besides  $a_k$  and  $b_k$ , which share a similar physical meaning, these parameters all have a distinctive, identifiable impact on the system thereby facilitating the tuning procedure. Moreover, this model can, to some extent, be regarded as a flow sensing-based hybrid approach between the classical DWM implementation and the standard, steady state speed deficit formulation. Its wake-particle formulation could further be considered analogous to the FLORIDyn tracking-points approach [13].

### 3. Numerical setup

The wake model predictions are compared to data recovered from high fidelity numerical simulations of a 15 NREL 5MW turbine [14] wind farm performed using an in-house fourth-order finite difference LES flow solver with improved actuator disks [15].

The studied wind farm layout is illustrated in Fig. 2 [16]: it consists of 3 rows of 5 wind turbines with a spacing of  $7D$  in each direction. The global dimensions of the simulation domain are  $54D \times 8D \times 32D$  and it is discretized using resolutions of 16 and 32 points per diameter in the lateral directions and vertical direction respectively, which results in a grid spacing of  $\Delta x = \Delta z = 7.875\text{m}$  and  $\Delta y = 3.975\text{ m}$ .

The spanwise direction is set to periodic and a rough wall law is applied on the bottom surface while a no-through flow condition is enforced at the top boundary. Finally, a concurrent precursor simulation is used to compute the inflow condition. The parameters of this precursor simulation are selected in order to obtain a hub height mean wind velocity of  $8\text{ ms}^{-1}$  and a moderate turbulence intensity of 6 %.

A wake tracking algorithm developed by Coudou [17] is applied to the 3D velocity field retrieved from this simulation in order to track the position of the wake centroid. This is achieved by finding the minimum of a convolution product between the available power density in the flow and a Gaussian masking function. The resulting wake centerline is plotted in black on Fig. 2.

The resulting high-fidelity flow data is compared to that obtained using the prediction provided by the wake model presented here. The operating parameters fed to the model are

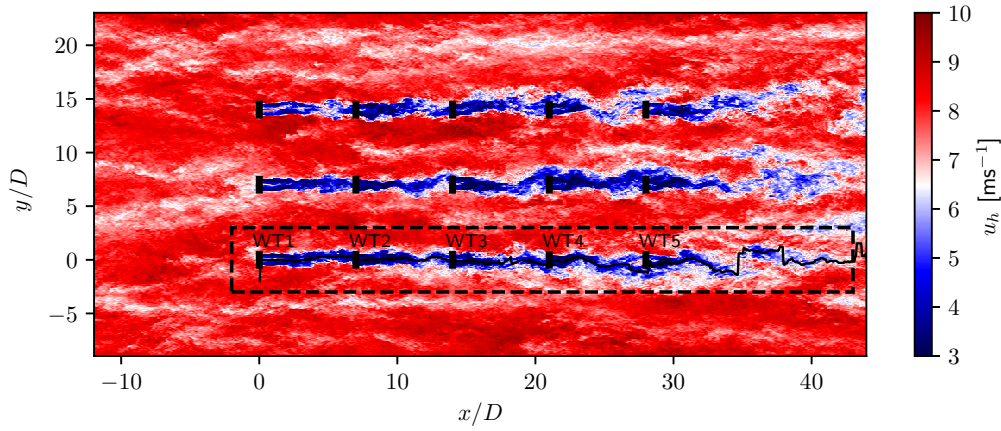


**Figure 2.** Streamwise velocity field measured at hub height extracted from the reference LES at  $t = 0$  s; position of the wake center as computed by the wake tracking algorithm (continuous black line) [16]

directly extracted from the LES output files while operating loads are computed on the same period based on the recovered disk forces saved at every time step of the simulation. The local flow field at the nacelle is probed by recovering the value of the transverse velocity directly from the LES data at the corresponding grid point.

#### 4. Results

In this section, the performances of the model developed are investigated and validated using the numerical setup described here above. Fig. 3 shows an instantaneous snapshot of the hub-height streamwise velocity field computed by the wake model along the first row of wind turbines (top) and compares it to the data extracted from the high-fidelity simulation (bottom). A good agreement is observed between these two approaches. The time responses of the two fields are similar and we can see on Fig. 3 that even though it only has access to limited, local, information, the wake model is able to consistently capture the main features of the wake in term of speed deficit and wake meandering. The small turbulent eddies, on the other hand, appear completely smoothed out. Due to the limited information available and simplified physics, reconstructing the full turbulent field is not achievable without the use of supplementary sensor device (LIDAR) and hence capturing the small turbulent eddies should not be expected using this approach.

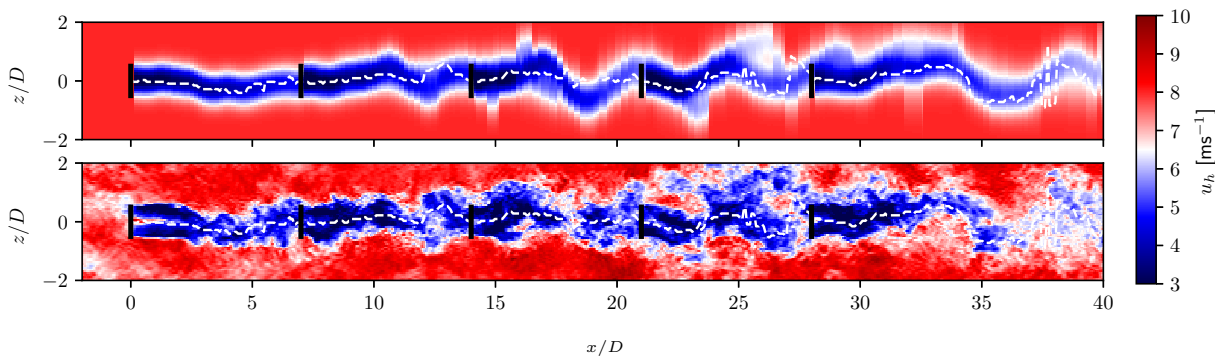


**Figure 3.** Instantaneous hub-height streamwise velocity field: model developed (top) and LES data (bottom) - wake center as computed from the high-fidelity simulation (dotted white line)

This is more quantitatively illustrated in Fig. 4, which shows that the model is also able to provide a consistent estimate of the position of the wake center even for waked turbines deep within the farm. Even though the time responses are mostly similar, we can still see that the model fails to capture some of the more abrupt wake centroid position variations predicted by the wake tracking algorithm. Examples of such discrepancies are visible at  $t = 360$  and  $560$  s for the fifth wind turbine of the row on Fig. 3 (bottom). It is however difficult to ascertain the reason for the latter discrepancies as they could originate from some intrinsic limitations of the model such as the smoothing introduced by the transverse velocity integrator but could also be traced down to inconsistencies in the tracking algorithm itself. Indeed the wake tracking algorithm was demonstrated to exhibit some inconsistent spikes as the wake becomes less coherent deep into the wind farm [16].

The results are finally compared in terms of their mean axial velocity profiles. The latter are plotted in Fig. 5. Since no near wake model is currently implemented, significant errors are observed in that region. As the wake propagates downstream, recovering its Gaussian shape in the process, the profile becomes increasingly similar. Wind turbines located deeper in the row experience a higher effective turbulent intensity, which eventually results in a faster wake recovery. In Fig. 5, we can see that the computation strategy of the wake growth constant effectively allows to capture this faster recovery for the downstream turbines.

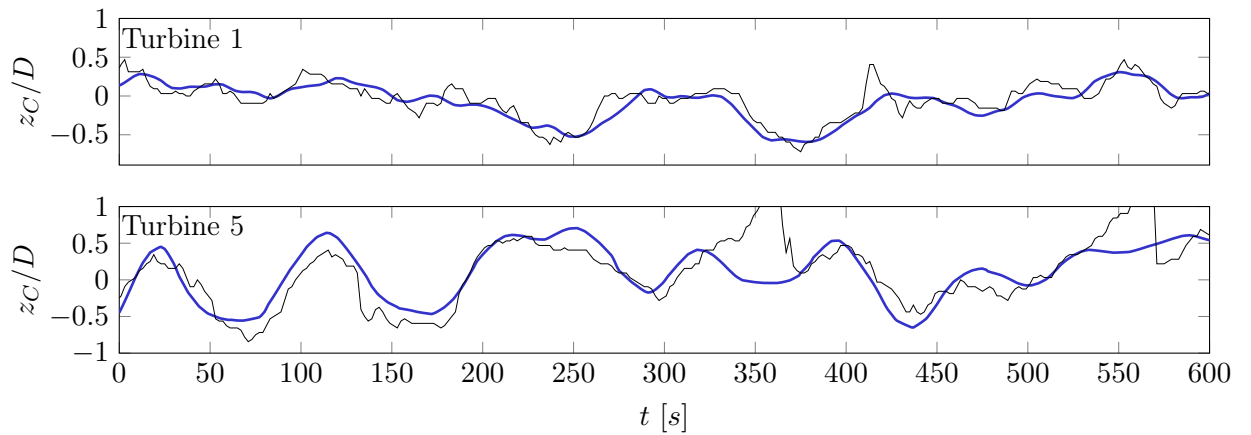


**Figure 4.** Comparison of the time evolution of the wake centroid position,  $z_C$ , as predicted by the model (thick blue) and as computed from the LES data (thin black) -  $z_C$  computed  $6D$  downstream the first wind (top) and last turbines (bottom) of the row

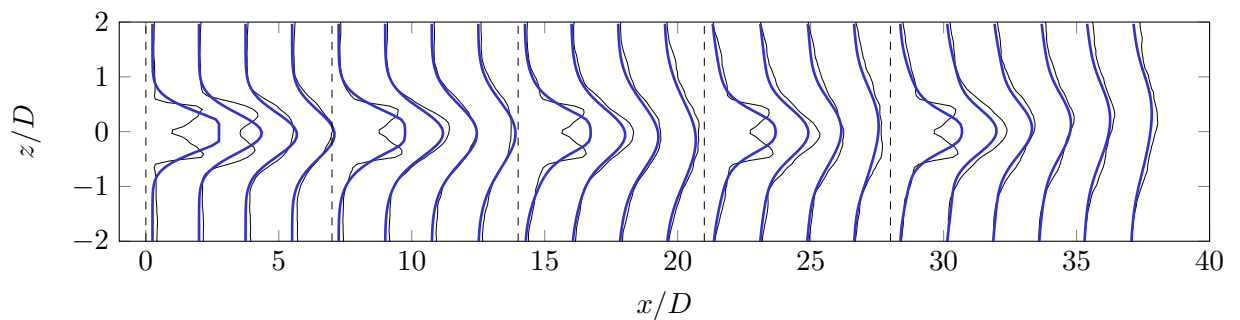


**Figure 5.** Comparison of the time-averaged axial speed deficit profiles computed by the model (thick blue) and by the LES data (thin black) - streamwise position of the wind turbines (thin dashed line)



## 5. Conclusions and perspectives

In this paper, we formulated an operational physics-based wake model combined with data assimilation fed by blade loads, wind probe measurements and turbine operating settings. A particular area for attention for the development of this model was the limitation of the number of input parameters and the reduction of the state space size in order to facilitate the tuning procedure. Preliminary comparisons against high-fidelity numerical simulations confirmed the good potential of the approach for online wake prediction within farms. This shall be confirmed by future validation studies under a wider range of operating conditions.

Beside this thorough model validation, further work shall include implementing a vortex based speed deficit formulation [18] along with investigating possible model correction strategies using sensors from downstream wind turbines impinged by the wake.

## Acknowledgments

This project has received funding from the European Research Council (ERC) under the European Union's Horizon 2020 research and innovation program (grant agreement no. 725627).

The present research benefited from computational resources made available on the Tier-1 supercomputer of the Fédération Wallonie-Bruxelles, infrastructure funded by the Walloon Region under the grant agreement no. 1117545.

## References

- [1] Jensen N 1983 A note on wind generator interaction Tech. rep. Risø National Laboratory
- [2] Bastankhah M and Porté-Agel F 2014 *Renewable Energy* **70** 116–123 URL <http://www.sciencedirect.com/science/article/pii/S0960148114000317>
- [3] Larsen G, Madsen Aagaard H, Bingöl F, Mann J, Ott S, Sørensen J, Okulov V, Troldborg N, Nielsen N, Thomsen K, Larsen T and Mikkelsen R 2007 *Dynamic wake meandering modeling* (Risø National Laboratory) ISBN 978-87-550-3602-4
- [4] Jonkman J M, Annoni J, Hayman G, Jonkman B and Purkayastha A 2017 *Development of FAST.Farm: A New Multi-Physics Engineering Tool for Wind-Farm Design and Analysis* (American Institute of Aeronautics and Astronautics) URL <https://doi.org/10.2514/6.2017-0454>
- [5] Fleming P A, Gebraad P M O, Churchfield M J, van Wingerden J W, Scholbrock A K and Moriarty P J 2014 Using particle filters to track wind turbine wakes for improved wind plant controls *2014 American Control Conference* pp 3734–3741
- [6] Iungo G V, Santoni-Ortiz C, Abkar M, Porté-Agel F, Rotea M A and Leonardi S 2015 *Journal of Physics: Conference Series* **625** 012009 ISSN 1742-6596 URL <http://dx.doi.org/10.1088/1742-6596/625/1/012009>
- [7] Gebraad P M O, Fleming P A and van Wingerden J W 2015 Wind turbine wake estimation and control using flordyn, a control-oriented dynamic wind plant model *2015 American Control Conference (ACC)* pp 1702–1708
- [8] Doekemeijer B, Boersma S, Pao L and van Wingerden J 2018 *Journal of Physics: Conference Series* **1037** 032013 URL <https://doi.org/10.1088/1742-6596/1037/2F032013>
- [9] Schreiber J, Bottasso C L, Salbert B and Campagnolo F 2019 *Wind Energy Science Discussions* **2019** 1–40 URL <https://www.wind-energ-sci-discuss.net/wes-2019-91/>
- [10] Bottasso C L, Cacciola S and Schreiber J 2018 *Renewable Energy* **116** 155–168 URL <http://www.sciencedirect.com/science/article/pii/S0960148117309072>
- [11] Duc T, Coupiac O, Girard N, Giebel G and Göçmen T 2019 *Wind Energy Science* **4** 287–302 URL <https://www.wind-energ-sci.net/4/287/2019/>
- [12] Doekemeijer B M, Van Wingerden J and Fleming P A 2019 A tutorial on the synthesis and validation of a closed-loop wind farm controller using a steady-state surrogate model *2019 American Control Conference (ACC)* pp 2825–2836 ISSN 0743-1619
- [13] Gebraad P M O and van Wingerden J W 2014 *Journal of Physics: Conference Series* **524** 012186 URL <https://doi.org/10.1088/1742-6596/524/2F012186>
- [14] JM J, Butterfield S, Musial W and Scott G 2009 *National Renewable Energy Laboratory (NREL)*
- [15] Moens M, Duponcheel M, Winckelmans G and Chatelain P 2018 *Wind Energy* **21** 766–782 (Preprint <https://onlinelibrary.wiley.com/doi/pdf/10.1002/we.2192>) URL <https://onlinelibrary.wiley.com/doi/abs/10.1002/we.2192>

- [16] Moens M, Coudou N and Chatelain P 2019 *Journal of Physics: Conference Series* **1256** 012012 URL <https://doi.org/10.1088/1742-6596/1256/1/012012>
- [17] Coudou N, Moens M, Marichal Y, Beeck J V, Bricteux L and Chatelain P 2018 *Journal of Physics: Conference Series* **1037** 072024 URL <https://doi.org/10.1088/1742-6596/1037/7/072024>
- [18] Marichal Y, Visscher I D, Chatelain P and Winkelmanns G 2017 *Journal of Physics: Conference Series* **854** 012030 URL <https://doi.org/10.1088/1742-6596/854/1/012030>